

TEMPORALLY PRECISE ACTION SPOTTING IN SOCCER VIDEOS USING DENSE DETECTION ANCHORS

João V. B. Soares Avijit Shah Topojoy Biswas

Yahoo Research

ABSTRACT

We present a model for temporally precise action spotting in videos, which uses a dense set of detection anchors, predicting a detection confidence and corresponding fine-grained temporal displacement for each anchor. We experiment with two trunk architectures, both of which are able to incorporate large temporal contexts while preserving the smaller-scale features required for precise localization: a one-dimensional version of a u-net, and a Transformer encoder (TE). We also suggest best practices for training models of this kind, by applying Sharpness-Aware Minimization (SAM) and mixup data augmentation. We achieve a new state-of-the-art on SoccerNet-v2, the largest soccer video dataset of its kind, with marked improvements in temporal localization. Additionally, our ablations show: the importance of predicting the temporal displacements; the trade-offs between the u-net and TE trunks; and the benefits of training with SAM and mixup.

Index Terms— Action detection, action spotting, dense detection, sharpness-aware minimization, u-net

1. INTRODUCTION

The *action spotting* task as proposed by Giancola et al. [1] aims to detect a single characteristic time instant for each action in a video. In the current paper, we tackle action spotting on SoccerNet-v2, which is currently the largest soccer dataset of its kind with respect to several important metrics [2].

One significant shortcoming of previous soccer action spotting approaches [3, 4, 5, 6, 7, 8, 9] is their imprecise temporal localization. While temporal localization errors may be acceptable when finding only the main events within soccer matches (which tend to have longer durations), there are a variety of applications where they become unacceptable. Examples include detecting scoring events in faster-paced sports, such as basketball and volleyball, as well as detecting frequent short events within soccer itself, such as *ball out of play*, and *throw-in* (the most frequent actions in SoccerNet-v2), or *passes* and *challenges*, which are not currently in SoccerNet-v2, but are highly relevant for sports analytics.

Our solution, illustrated in Fig. 1, makes use of a dense set of detection anchors. We define an anchor for every pair formed by a time instant (usually taken every 0.5 or 1.0 sec-

onds) and action class, thus adopting a multi-label formulation. For each anchor, we predict both a detection confidence and a fine-grained temporal displacement. This approach leads to a new state-of-the-art on SoccerNet-v2. Experiments show large improvements in temporal precision, with substantial benefits from the temporal displacements.

Our approach is inspired by work in object detection. In particular, Lin et al. [10] demonstrated the advantages of using a dense set of detection anchors, with their single-stage RetinaNet detector surpassing the accuracy of slower contemporary two-stage counterparts. One important difference here is that the output space for action spotting is inherently lower-dimensional than that of object detection, given that each action can be completely defined by its time and class. This allows us to use a very dense set of action spotting anchors, at a relatively much lower computational cost.

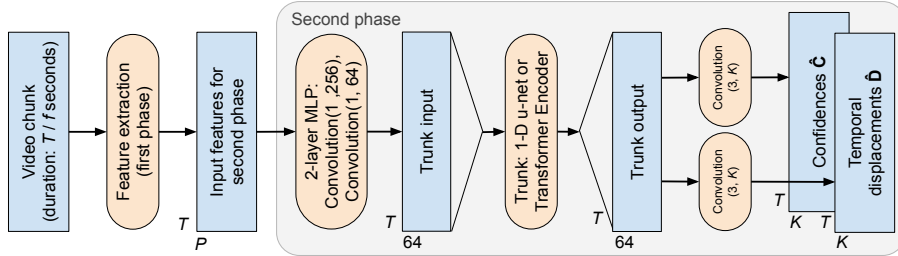
For the trunk of our models, we experiment with a one-dimensional version of a u-net [11] as well as a Transformer encoder [12]. Both architectures incorporate large temporal contexts important for action spotting, while also preserving the smaller-scale features required for precise localization. We show that, while both architectures can achieve good results, the u-net has a better trade-off of time and accuracy.

The SoccerNet-v2 dataset is of moderate size, containing around 110K action spotting labels. At the same time, deep networks generally require large amounts of data or pre-training strategies to work well in practice. We show that Sharpness-Aware Minimization (SAM) [13] and mixup data augmentation [14] are able to improve results significantly on the dataset, thus mitigating the lack of larger scale data.

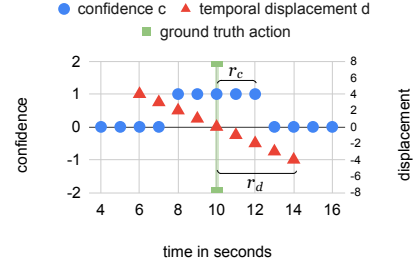
2. RELATED WORK

Since the release of the SoccerNet datasets [1, 2], several action spotting methods have been proposed [3, 4, 5, 6, 7, 8, 9].

Related to our approach, RMS-Net [3] and CALF [4] also use temporal regression, but with very different formulations. RMS-Net [3] predicts at most one action per video chunk, and makes use of a max-pooling operation over the whole temporal dimension. It is thus not well suited for predicting multiple nearby actions. This differs from the CALF model [4], which produces a set of possible action predictions per video chunk, each of which may correspond to any time instant within the



(a) Architecture overview



(b) Targets around a ground-truth action

Fig. 1: (a) Architecture overview, where Convolution(w, n) denotes a convolution with kernel size w and n filters. (b) Example of target confidences $c_{*,k}$ and temporal displacements $d_{*,k}$ for a single class k , around a ground-truth action of the same class, at one anchor per second. Note temporal displacement targets are undefined outside of the radius r_d of the ground-truth action.

chunk, and belong to any class. The model is thus faced with a challenging problem to learn: simultaneously assigning all of its predictions to time instants and classes such that, in the aggregate, they cover all existing actions within the chunk. Our dense anchor approach sidesteps this challenge, by having each output anchor being preassigned to a time instant and class. This naturally allows for predicting multiple actions per video chunk while using large chunk sizes that provide ample context for prediction. Our regressed temporal displacements are then used to further finely localize each action in time.

Zhou et al. [7] presented experiments using a Transformer Encoder (TE) on SoccerNet-v2. Differently from their work, our approach makes use of the encoder output at every token, which is used to generate predictions for our dense set of anchors. In addition, here we also experiment with a one-dimensional version of a u-net, and show that it has a better trade-off of time and accuracy relative to the TE.

3. METHODS

Following previous works [2, 3, 4, 6, 7], we adopt a two-phase approach to action spotting, consisting of feature extraction followed by action prediction. This significantly decreases the computational burden during training and also allows us to perform meaningful comparisons across methods. We note, however, that training end-to-end [3] and fine-tuning feature extraction backbones [7] have both shown to further improve results and represent promising directions for future work.

Our two-phase architecture is illustrated in Fig. 1(a). In the first phase, a video chunk is decoded into frames, from which a sequence of T feature vectors of dimension P is extracted, composing a $T \times P$ feature matrix. In the second phase, this matrix is used to produce the action predictions. This starts with a single two-layer MLP applied independently to each input feature vector, resulting in a lower-dimensional output, which then gets fed into the model’s trunk. As described in 3.2, the trunk combines information across all temporal locations while maintaining the sequence size T . As described in 3.1, the trunk’s output is used to cre-

ate predictions for the dense set of $T \times K$ anchors, with K the number of classes. When training, our loss is applied directly to all anchor predictions, while at test-time, post-processing is used to consolidate them into a set of action detections.

3.1. Dense detection anchors

We use a dense set of detection anchors, inspired by dense single-stage object detectors [10]. The output from our model’s trunk is attached to two heads, predicting respectively confidences $\hat{\mathbf{C}} = (\hat{c}_{t,k})$ and temporal displacements $\hat{\mathbf{D}} = (\hat{d}_{t,k})$, where $t = 1, 2, \dots, T$ indexes the T temporal locations of a given video chunk, and $k = 1, 2, \dots, K$ indexes the K classes. $\hat{\mathbf{C}}$ and $\hat{\mathbf{D}}$ are computed from the trunk outputs via their respective convolution operations, each using a temporal window of size 3 and having K output channels.

We define a confidence loss L_c and a temporal displacement loss L_d , training a separate model for each rather than optimizing them jointly (see Section 3.3). The losses are computed with respect to *targets* (desired outputs), which are derived from the N ground-truth actions contained within the given video chunk, which we denote $G = \{(t_i, k_i)\}_{i=1}^N$. These targets, illustrated in Fig. 1(b), are described below.

The confidence loss L_c for a video chunk is computed with respect to target confidences $\mathbf{C} = (c_{t,k})$, defined to be 1 within a r_c seconds radius of a ground-truth action and 0 elsewhere, i.e. $c_{t,k} = I(\exists(s, k) \in G: |s - t| \leq r_c f)$, where I is the indicator function and f is the temporal feature rate (the number of feature vectors extracted per second). The confidence loss is defined as $L_c(\hat{\mathbf{C}}, \mathbf{C}) = \sum_{k=1}^K \sum_{t=1}^T \text{CE}(\hat{c}_{t,k}, c_{t,k})$, where CE denotes the standard cross-entropy loss. We found that r_c on the order of a few seconds gave the best results. This entails a loss in temporal precision, as the model learns to output high confidences within the whole radius of when an action actually happened, motivating the use of the temporal displacement outputs $\hat{\mathbf{D}}$. As we show in experiments, incorporating the displacements results in a large improvement to temporal precision.

The temporal displacement loss L_d is only applied within

an r_d seconds radius of ground-truth actions, given that predicted displacements will only be relevant when paired with high confidences. Thus, for each class k , we first define its temporal support set $S(k) = \{t = 1, 2, \dots, T \mid \exists(s, k) \in G: |s - t| \leq r_d f\}$. We then define the loss $L_d(\hat{\mathbf{D}}, \mathbf{D}) = \sum_{k=1}^K \sum_{t \in S(k)} L_h(\hat{d}_{t,k}, d_{t,k})$, where L_h denotes the Huber regression loss and the targets $\mathbf{D} = (d_{t,k})$ are defined so that each $d_{t,k}$ is the signed difference between t and the temporal index of its nearest ground-truth action of class k in G .

At test-time, to consolidate the predictions from $\hat{\mathbf{C}}$ and $\hat{\mathbf{D}}$, we apply two post-processing steps. The first displaces each confidence $\hat{c}_{t,k}$ by its corresponding displacement $\hat{d}_{t,k}$, keeping the maximum confidence when two or more are displaced into the same temporal location. The second step applies non-maximum suppression (NMS) [1, 6] to the displaced confidences. Since we adopt a multi-label formulation, we apply NMS separately for each class. To demonstrate the improvement from incorporating the temporal displacements, we later present an ablation where they are ignored, which is done simply by skipping the first post-processing step above. Note we do not apply any post-processing during training, instead defining the losses directly on the raw model predictions.

3.2. Trunk architectures

We experiment with two different trunk architectures. The first is a 1-D version of a u-net [11]. The u-net consists of a contracting path that captures global context, followed by a symmetric expanding path, whose features are combined with those from the contracting path to enable precise localization. We replace the u-net’s standard 2-D convolution blocks with 1-D versions of ResNet-V2 bottleneck blocks [15], which gave improved results while stabilizing training.

The second trunk architecture we experiment with is a Transformer encoder (TE) [12], whose attention mechanism allows each token in a sequence to attend to all other tokens, thus incorporating global context while still preserving important local features. Relative to convolutional networks such as the u-net, Transformers have less inductive bias, often requiring pretraining on large datasets, or strong data augmentation and regularization [16, 17, 18]. Here, we achieve good results with the TE by training with Sharpness-Aware Minimization (SAM) [13] and mixup [14], as described in Section 3.3.

3.3. Training

We train our models from scratch using the Adam optimizer with Sharpness-Aware Minimization (SAM) [13], mixup data augmentation [14], and decoupled weight decay [19]. SAM seeks wide minima of the loss function, which has been shown to improve generalization [13], in particular for small datasets and models with low inductive bias [16]. We do not apply batch normalization when training the u-net, finding that its skip connections were sufficient to stabilize training.

We found it convenient to train temporal displacement regression separately from confidence prediction, resulting in a two-step approach. This provides similar results to joint training, while simplifying experimental design. We first train a model that produces only confidences, by optimizing the confidence loss L_c and making use of mixup data augmentation [14]. We then train a second model that produces only temporal displacements, by optimizing L_d , but *without* applying mixup. Due to the temporal displacement loss only being defined within small windows around ground-truth actions, we found it difficult to effectively apply mixup when using it.

4. EXPERIMENTS

4.1. Experimental Settings

We present results on two sets of features. The first consists of ResNet-152 features extracted at $f = 2$ fps [2]. We experiment with the PCA version, here denoted ResNet+PCA. The second set comes from a series of models fine-tuned on SoccerNet-v2 [7], which we denote as Combination, whose features are extracted at $f = 1$ fps. Our two-layer MLP has layers with respectively 256 and 64 output channels, generating a $T \times 64$ matrix irrespective of the input feature set size.

We experimentally chose a chunk size of 112s and radii for the confidence and displacement targets of $r_c = 3$ s and $r_d = 6$ s. We use an NMS suppression window of 20s, following previous works [6, 7]. Training and inference speeds were measured using wall times on a cloud instance with a V100 vGPU, 48 vCPUs at 2.30GHz, and 256GiB RAM.

At each contracting step of the u-net, we halve the temporal dimension while doubling the channels. Expansion follows a symmetric design. We contract and expand 5 times when using ResNet+PCA ($T = 224$), and 4 times when using Combination features ($T = 112$), so in both cases the smallest temporal dimension becomes $224/2^5 = 112/2^4 = 7$.

We experiment with two sizes for the TE: Small and Base. Small has 4 layers, embedding size 128, and 4 attention heads, while Base has 12 layers, embedding size 256 and 8 attention heads. Due to GPU memory limitations, we use a batch size of 64 for Base, while Small uses our default of 256.

For each model, we choose a set of hyper-parameters on the validation set. To decrease costs, we optimize each hyper-parameter in turn, in the following order: the learning rate; SAM’s ρ (when applicable); the weight decay; and the mixup α (when applicable). We use a batch size of 256 and train for 1,000 epochs, where each epoch consists of 8,192 uniformly sampled video chunks. We apply a linear decay to the learning rate and weight decay, so that the final decayed values (at epoch 1,000) are 1/100th of the respective initial values. We train each model five times and report average results.

We report results on SoccerNet’s average-mAP metric, which uses tolerances $\delta = 5, 10, \dots, 60$ s, as well as the recent *tight* average-mAP metric, which uses $\delta = 1, 2, 3, 4, 5$ s [20].

Method	Features	Avg.-mAP	Chunks/second	Epoch time	Params
DU	RN+PCA	63.8	1,447	5.4s	17.5M
DU+SAM	RN+PCA	72.0	1,447	8.1s	17.5M
DU+SAM+mixup	RN+PCA	72.2	1,447	8.3s	17.5M
DTEB+SAM+mixup	RN+PCA	68.2	1,329	15.0s	1.0M
DTEB+SAM+mixup	RN+PCA	72.4	342	112.0s	9.7M
DU	Combin.	75.7	511	13.7s	8.9M
DU+SAM	Combin.	76.1	511	18.4s	8.9M
DU+SAM+mixup	Combin.	77.3	511	22.7s	8.9M

Table 1: Ablations exploring different feature sets, model trunks, and the use of SAM and mixup. Chunks/second measures each model’s inference throughput, excluding first-stage feature extraction and all post-processing.

The tolerance δ defines the time difference allowed between a detection and a ground-truth action such that the detection may still be considered a true positive. Thus, smaller tolerances enforce a higher temporal precision. Note δ is unrelated to the radii r_c and r_d , the latter only used during training.

4.2. Results

A set of ablations is presented in Table 1, where DU, DTEB and DTEB stand for the dense anchor model using respectively the u-net, Small TE and Base TE. We see a large improvement when applying SAM with the ResNet+PCA features, but a very small one when it is applied with the Combination features, which were already fine-tuned on the same dataset. Mixup gives small improvements across both feature types. DTEB+SAM+mixup achieves average-mAP similar to that of DU+SAM+mixup, but with a much longer training time and lower throughput. Recent techniques have reduced the computational demands of Transformers [21], while pre-training is well-known to improve their results [16, 17, 18], though we have not currently explored those directions.

Results comparing methods across various tolerances δ are presented in Figure 2. We include results from CALF [4] and NetVLAD++ [6], whose implementations were made available by their authors. All results in the figure were generated using the ResNet+PCA features. While our method outperforms the previous approaches across all tolerances, the improvement is significantly larger at smaller ones. The figure also shows that the temporal displacements provide significant improvements at small matching tolerances, without affecting results at larger ones. This observation is confirmed in Table 2, where our method without the temporal displacements \hat{D} has much lower tight average-mAP.

Comparisons to prior work are presented in Table 2. On the ResNet+PCA features, DU outperforms CALF [4] and NetVLAD++ [6]. Surprisingly, DU+SAM+mixup on the same set of features outperforms other methods that use fine-tuned features, excluding that of Zhou et al. [7]. When we apply our model on Zhou et al.’s pre-computed features, we see substantial improvements. In general, our model’s

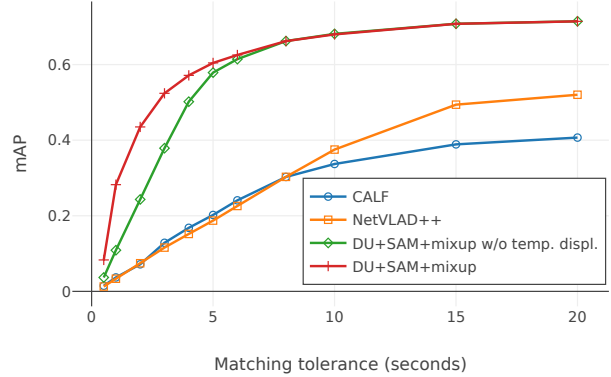


Fig. 2: mAP for different methods, as a function of the matching tolerance δ . While the standard average-mAP metric is defined with tolerances of up to 60 seconds, the graph focuses on smaller tolerances, of up to 20 seconds.

Method	Features	A-mAP	Tight a-mAP
NetVLAD++ [6]	ResNet	53.4	11.5*
AImageLab RMSNet [3]	ResNet-tuned	63.5*	28.8*
Vis. Analysis of Humans	CSN-tuned	64.7†	46.2†
CALF [2, 4]	ResNet+PCA	40.7	12.2‡
NetVLAD++ [6]	ResNet+PCA	50.7	11.3‡
DU	ResNet+PCA	63.8	41.7
DU+SAM+mixup w/o \hat{D}	ResNet+PCA	72.1	39.3
DU+SAM+mixup	ResNet+PCA	72.2	50.7
Zhou et al. [7]	Combination	73.8	47.1*
DU	Combination	75.7	58.5
DU+SAM+mixup w/o \hat{D}	Combination	77.3	46.8
DU+SAM+mixup	Combination	77.3	60.7

Table 2: Comparison with results from prior works. * Results reported on challenge website [20]. † Results reported on challenge website for the *challenge* split, whereas all other reported results are on the standard *test* split. ‡ Results computed using the implementation provided by the authors.

improvements are larger on the tight average-mAP metric.

5. CONCLUSION

This work presented a temporally precise action spotting model that uses a dense set of detection anchors. The model sets a new state-of-the-art on SoccerNet-v2 with marked improvements when evaluated at smaller tolerances. For the model’s trunk, we experimented with a 1-D u-net as well as a TE, showing that the TE requires a much larger computational budget to match the accuracy of the u-net. Ablations demonstrated the importance of predicting fine-grained temporal displacements for temporal precision, as well as the benefits brought by training with SAM and mixup data augmentation.

Acknowledgements We are grateful to Gaurav Srivastava for helpful discussions and for reviewing this manuscript.

6. REFERENCES

- [1] Silvio Giancola, Mohieddine Amine, Tarek Dghaily, and Bernard Ghanem, “SoccerNet: A scalable dataset for action spotting in soccer videos,” in *Computer Vision and Pattern Recognition (CVPR) Workshops*, 2018.
- [2] Adrien Deliege, Anthony Cioppa, Silvio Giancola, Meisam Seikavandi, Jacob Dueholm, Kamal Nasrollahi, Bernard Ghanem, Thomas Moeslund, and Marc Van Droogenbroeck, “SoccerNet-v2: A dataset and benchmarks for holistic understanding of broadcast soccer videos,” in *Computer Vision and Pattern Recognition (CVPR) Workshops*, 2021, pp. 4508–4519.
- [3] Matteo Tomei, Lorenzo Baraldi, Simone Calderara, Simone Bronzin, and Rita Cucchiara, “RMS-Net: Regression and masking for soccer event spotting,” in *International Conference on Pattern Recognition (ICPR)*, 2021.
- [4] Anthony Cioppa, Adrien Deliege, Silvio Giancola, Bernard Ghanem, Marc Van Droogenbroeck, Rikke Gade, and Thomas Moeslund, “A context-aware loss function for action spotting in soccer videos,” in *Computer Vision and Pattern Recognition (CVPR)*, 2020.
- [5] Anthony Cioppa, Adrien Deliege, Floriane Magera, Silvio Giancola, Olivier Barnich, Bernard Ghanem, and Marc Van Droogenbroeck, “Camera calibration and player localization in SoccerNet-v2 and investigation of their representations for action spotting,” in *Computer Vision and Pattern Recognition (CVPR) Workshops*, 2021, pp. 4537–4546.
- [6] Silvio Giancola and Bernard Ghanem, “Temporally-aware feature pooling for action spotting in soccer broadcasts,” in *Computer Vision and Pattern Recognition (CVPR) Workshops*, 2021.
- [7] Xin Zhou, Le Kang, Zhiyu Cheng, Bo He, and Jingyu Xin, “Feature combination meets attention: Baidu soccer embeddings and Transformer based temporal detection,” *arXiv preprint arXiv:2106.14447*, 2021.
- [8] Bastien Vanderplaetse and Stephane Dupont, “Improved soccer action spotting using both audio and video streams,” in *Computer Vision and Pattern Recognition (CVPR) Workshops*, 2020, pp. 896–897.
- [9] Kanav Vats, Mehrnaz Fani, Pascale Walters, David A Clausi, and John Zelek, “Event detection in coarsely annotated sports videos via parallel multi-receptive field 1d convolutions,” in *Computer Vision and Pattern Recognition (CVPR) Workshops*, 2020, pp. 882–883.
- [10] Tsung-Yi Lin, Priya Goyal, Ross Girshick, Kaiming He, and Piotr Dollár, “Focal loss for dense object detection,” in *International Conference on Computer Vision*, 2017.
- [11] Olaf Ronneberger, Philipp Fischer, and Thomas Brox, “U-net: Convolutional networks for biomedical image segmentation,” in *International Conference on Medical image computing and computer-assisted intervention (MICCAI)*. Springer, 2015, pp. 234–241.
- [12] Ashish Vaswani, Noam Shazeer, Niki Parmar, Jakob Uszkoreit, Llion Jones, Aidan Gomez, Łukasz Kaiser, and Illia Polosukhin, “Attention is all you need,” in *Advances in neural information processing systems*, 2017.
- [13] Pierre Foret, Ariel Kleiner, Hossein Mobahi, and Behnam Neyshabur, “Sharpness-aware minimization for efficiently improving generalization,” in *International Conference on Learning Representations*, 2021.
- [14] Hongyi Zhang, Moustapha Cisse, Yann N. Dauphin, and David Lopez-Paz, “mixup: Beyond empirical risk minimization,” in *International Conference on Learning Representations (ICLR)*, 2018.
- [15] Kaiming He, Xiangyu Zhang, Shaoqing Ren, and Jian Sun, “Identity mappings in deep residual networks,” in *European conference on computer vision (ECCV)*, 2016.
- [16] Xiangning Chen, Cho-Jui Hsieh, and Boqing Gong, “When Vision Transformers outperform ResNets without pre-training or strong data augmentations,” in *International Conference on Learning Representations (ICLR)*, 2022.
- [17] Jacob Devlin, Ming-Wei Chang, Kenton Lee, and Kristina Toutanova, “BERT: Pre-training of deep bidirectional transformers for language understanding,” in *North American Association for Computational Linguistics (NAACL)*, 2019, pp. 4171–4186.
- [18] Alexey Dosovitskiy, Lucas Beyer, Alexander Kolesnikov, Dirk Weissenborn, Xiaohua Zhai, Thomas Unterthiner, Mostafa Dehghani, Matthias Minderer, Georg Heigold, Sylvain Gelly, Jakob Uszkoreit, and Neil Houlsby, “An image is worth 16x16 words: Transformers for image recognition at scale,” in *International Conference on Learning Representations (ICLR)*, 2021.
- [19] Ilya Loshchilov and Frank Hutter, “Decoupled weight decay regularization,” in *International Conference on Learning Representations (ICLR)*, 2019.
- [20] “SoccerNet action spotting challenge description and results,” <https://github.com/SoccerNet/sn-spotting>, 2021, Accessed: February, 2022.
- [21] Yi Tay, Mostafa Dehghani, Samira Abnar, Yikang Shen, Dara Bahri, Philip Pham, Jinfeng Rao, Liu Yang, Sebastian Ruder, and Donald Metzler, “Long range arena : A benchmark for efficient Transformers,” in *International Conference on Learning Representations (ICLR)*, 2021.